SAW Phononic Reflector Structures

N. Y. Kozlovski and D. C. Malocha
School of Electrical Engineering and Computer Science
University of Central Florida, Orlando, Florida 32816

Abstract— **This paper will present theory, analysis and experimental work on SAW phononic reflector structures. The term SAW phononic structures is used since the structures are composed of a-periodic or pseudo-periodic structures that are designed to affect the propagation of surface acoustic waves in a manner similar to the periodic potential in a semiconductor which affects the electron's energy in allowed or forbidden bands based on the crystal material. The simplest SAW reflective structure commonly used is the synchronous reflector, which provides a very narrow frequency stop-band. By building varying one-dimensional structures in the SAW propagation direction, it is possible to control and design numerous pass- and stop-bands, which provides frequency dependent transmission or reflection, and span large fractional bandwidths, unlike the simple SAW Bragg reflector. These types of a-periodic and pseudo-periodic structures have not been previously shown in the literature and may provide the possibilities of new SAW device embodiments.**

This work will discuss the basic theory which we use in the design of the phononic reflective structures. The approach uses the concept of orthogonal frequencies that allows the building of the a-periodic or pseudo-periodic structures. It is possible to design and predict various a-periodic structure performance quite well using an intuitive model. A coupling of modes (COM) model is then used to simulate the complex structure, and predict the overall frequency dependent reflectance or transmittance of the structure. The time domain COM responses can also be predicted and compared to the intuitive approach to provide insight. As expected, allowed and unallowed frequency bands are present. By changing the structures, the band characteristics can be changed in a predictive manner over a wide bandwidth.

Experimental devices at 250MHz are built on YZ $LiNbO_3$to demonstrate the SAW phononic structures and to confirm model predictions. The paper will present several phononic structures, theoretical analysis and simulations, and compare the predicted and measured results.

I. Introduction

Nature has provided numerous examples of its use of periodic, pseudo-periodic and aperiodic structures to attain certain desired properties. One example is the definition of an electronic material as single-crystal (periodic), poly-crystalline (pseudo-periodic) or amorphous (aperiodic). In a material, such as a semiconductor, the structure has a profound effect on the material properties and movement of an electron through the material. The effect of a material structure on the electron propagation has an analogy to light properties propagating in certain optical structures, which has been termed photonic materials or structures. The same analogy is true for an acoustic mode propagating in certain structures, termed a phononic structure.

Previous works have analyzed or showed initial results of wave propagation in phononic crystals. Some work has focused on creation of acoustic band gaps in phononic crystals [1]–[4], guiding of waves using phononic crystals has been experimentally demonstrated [5], [6], and SAW effects in phononic structures has been studied [7]–[9]. Nelin described phase apodization in crystals to generate a phononic structure response, which may also have application in future phononic SAW structures [7]. Dhar and Rogers used lithography to fabricate phononic structures on crystals [10].

This paper will introduce a study of some SAW phononic structures and their SAW propagation properties. The structures will consist of periodic, pseudo-periodic and aperiodic reflectors which have interesting frequency and time domain characteristics. It is possible to produce some new and unique one dimensional phononic structures using similar concepts developed for orthogonal frequency coded (OFC) SAW devices [11]. The paper will provide definitions of the structures, a basic theory and predictions based on a coupling of modes (COM) formulation. Experimental results of devices fabricated on YZ $LiNbO_3$will be compared to theoretical predictions.

II. Definitions and Theory

In order to describe the various reflector structures discussed, some definitions will be introduced.

- The most basic structure, which we will define as the primitive cell, is composed of an electrode and a gap, as shown in Fig. 1.
- A unit cell is the smallest repetitive structure in the entire reflector.
- A periodic structure is one where the unit cell is repeated multiple times with period p. In an OFC device, a chip contains multiple primitive cells and is a perfectly periodic structure.
- Combining multiple chips having differing periods (or local frequencies) in an OFC reflector creates a pseudo-periodic structure, which has been termed a bit.
- An aperiodic reflector is composed of multiple primitive cells which have random periods. The primitive may, or may not, be used multiple times within the reflector.
- A super cell is composed of identical multiple unit cells, which are repeated periodically.

Fig. 1 shows the definition of an i^{th} primitive cell. Each electrode has its own bounding box of width p_i, electrodes width is a_i and is offset within the bounding box by d_i. Parameter x_i defines the spacing between bounding boxes of the $(i-1)^{th}$ and i^{th} electrodes.

To obtain a simple understanding of what is expected, a first order mathematical analysis is considered, which ignores the acoustic implementation. Given a the unit cell structure with

1-4244-0647-1/07/$20.00 ©2007 IEEE

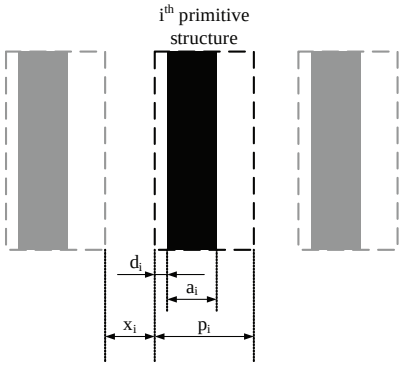

Fig. 1. Definition of primitive SAW structure

a time response $h(t)$, and a frequency response $H(f)$, having a time length τ_B and repeated N times, then $h_N(t)$ is given as

$$h_N(t) = \sum_{n=0}^{N-1} h(t + \tau_B \cdot n) \tag{1}$$

The frequency response $H_N(f)$ is

$$H_N(f) = \sum_{n=0}^{N-1} H(f)\, e^{-j(4\pi \cdot f \cdot \tau_B)n} \tag{2}$$

Defining

$$\alpha(f) = 4\pi \cdot f \cdot \tau_B \tag{3}$$

equation (2) can be reduced to

$$H_N(f) = H(f) \sum_{n=0}^{N-1} \left[e^{-j\cdot\alpha(f)}\right]^n \tag{4}$$

The summation in equation 4 is recognized as a geometric progression and using the summation formula for such a progression, equation (4) yields

$$H_N(f) = H(f) \cdot \frac{1 - e^{-j\cdot N\cdot\alpha(f)}}{1 - e^{-j\cdot\alpha(f)}} \tag{5}$$

Factoring out the exponents, applying Euler's formula, and back substituting using equation (3), $H_N(f)$ can be expressed as a product, rewritten as

$$H_N(f) = H(f)\, e^{-j\cdot(N-1)\cdot 2\pi\cdot f\cdot\tau_B} \frac{sin(N \cdot 2\pi \cdot f \cdot \tau_B)}{sin(2\pi \cdot f \cdot \tau_B)} \tag{6}$$

The peak frequencies are

$$2\pi \cdot f_{peak} \cdot \tau_B = m_1 \cdot \pi \tag{7}$$

where $m_1 \in \mathbb{N}$

$$f_{peak} = \frac{m_1}{2 \cdot \tau_B} \tag{8}$$

The relationship to the frequency nulls is

$$N \cdot 2\pi \cdot f_{null} \cdot \tau_B = m_2 \cdot \pi \tag{9}$$

where $m_2 \in \left\{\mathbb{N} : \frac{N}{m_2} \notin \mathbb{N}\right\}$

$$f_{null} = \frac{m_2}{2 \cdot \tau_B \cdot N} \tag{10}$$

The null bandwidth is given as

$$BW_{null} = \frac{N \cdot m_3 + 1}{2 \cdot \tau_B \cdot N} - \frac{N \cdot m_3 - 1}{2 \cdot \tau_B \cdot N} = \frac{1}{\tau_B \cdot N} \tag{11}$$

$H_N(f)$ is expressed as a product of $H(f)$, which is the unit cell frequency response, a linear phase term of unity magnitude, and a real, modulating function. Fig. 2 is an example response of $H_N(f)$, for $N = 2, 3, 4$ and $H(f) = 1$. Expressions for peak and null locations and peak bandwidth are given in equations (8), (10), and (11), respectively.

This simple analysis is applicable to idealized short reflector arrays. It assumes the inter- and intra-reflections are negligible and that the electrode reflection is approximately equal to a half-wavelength at the local carrier frequency, or where the period is $^1/_2$ wavelength. This is not always true, as will be demonstrated, but it provides an understanding of what is expected and a direction for experimentation. As seen in Fig. 2, a series of periodic stop bands will be produced due to the multiple periodic unit cells creating the super cell. This would correspond to the idealized reflector response of such a structure. By changing the unit cell and/or super cell, differing stop (reflection) and pass bands can be achieved. This is simple analysis needs to be extended using the COM analysis and to show experimental verification.

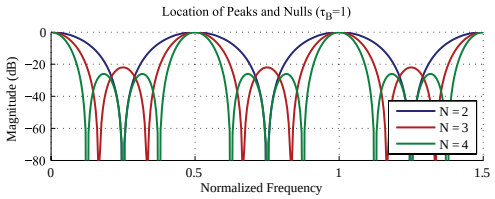

Fig. 2. Example of normalized magnitude frequency response from simple model calculations for super cells with 2, 3 and 4 unit cells. As N increases, the local stopband frequencies narrow. The effects of increased reflectivity and inter- and intra- reflector interactions are not predicted in the simple model.

III. Test Devices

A total of eight devices were modeled, built, and tested. All of the devices were one-port devices and had a $3 \cdot f_0$ apodized transducer which reduced second order transducer effects. To verify the theory developed in section II, an OFC structure was initially chosen as a unit cell for its well behaved and slowly changing frequency response, $H(f)$. This response should give us good verification of peak and null locations and predicted bandwidth. A 3-chip OFC structure was designed to have frequencies 245.2MHz, 250.0MHz, and 254.8MHz with 25, 26 and 27 electrodes respectively. Super cells were built from OFC bits repeated 1, 2, 3, and 4 times

as show in Fig. 3. Devices were then labeled as OFC x1, OFC x2, and so on. Primitive structures were designed which have $p_i = 0.5\lambda_i$, $x_i = d_i = 0$, and $a_i = 0.25\lambda_i$, where λ_i is corresponding wavelength to each frequency.

Also a random structure was used as a unit cell for a second set of four devices. This structure was built using the primitive cells from the previously described OFC structure. Primitive structures (electrode followed by free space each of quarter wavelength width) were randomly shifted within the unit cell, yielding the same total number of electrodes and length of the unit cell as described for OFC. This unit cell was then repeated similarly to the OFC xN devices; 1, 2, 3 and 4 times as shown in Fig. 4, and labeled RND x1, RND x2, and so on.

The second set of random and pseudo-random devices provided a unique reflectivity response and was also used to examine the accuracy of the COM model when simulating fast changing structures. The COM model has been shown to be accurate for slowly varying changes in electrode periodicity. The random unit cell structure can have rapidly changing primitive cell characteristics, which can challenge the applicability of the COM model.

IV. Models

Two models were used to design and predict the device response. The simple model was primarily used to provide an analytic design tool; it has simple equations and gives the ability to develop design algorithms. The reflector response is approximated by idealized time carriers dependent on the period of the electrode modeled. It does not take under consideration coupling, inter-reflectivity, and second order effects. Reflection is linearly proportional to the number of electrodes and does not model the stored energy.

For a more complete analysis which includes coupling, inter-reflectivity and second order effects, the COM model is applied to the structures [12].

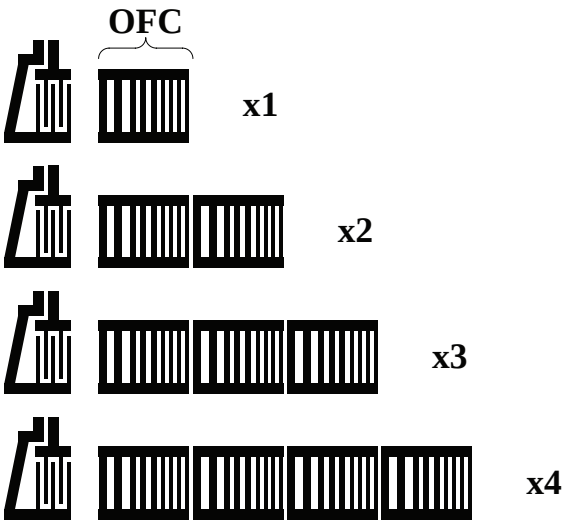

Fig. 3. OFC bit device layouts (drawing is not to scale, nor does it show the correct number of electrodes), structures. Because there can be defined a unit cell which is repeated within the structure, the structure is pseudo-periodic.

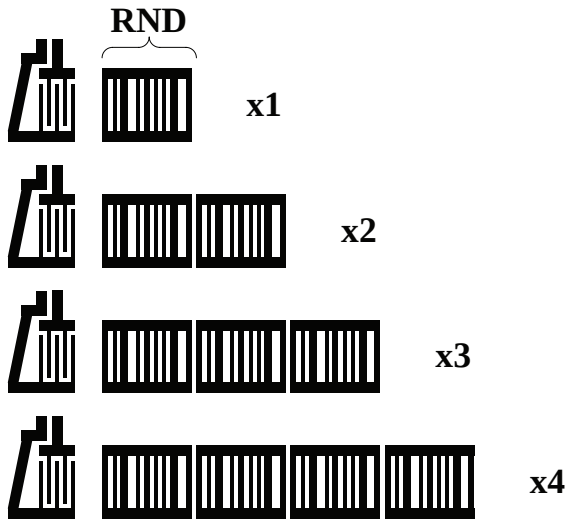

Fig. 4. Random bit device layouts (drawing is not to scale, nor does it show correct number of electrodes). For device RNDx1, the unit cell consists of totally random primitive cells, but the super cells in the other devices is pseudo-random, consisting of RNDx1 periodically used in the super cell.

Both models define one primitive structure (electrode) at a time. Also, both models produce the expected reflective S-parameter of the acoustic ports. Acoustic ports cannot be measured directly, which requires transducers for launching and receiving the SAW and their effect needs to be compensated when extracting the data.

Fig. 5 shows the COM model predicted frequency response of OFC x1 through OFC x4 devices. Peaks, nulls, and bandwidth correlate well with theory developed in section II. In this case the bit length τ_B is approximately .9μs. As expected, the unit cell response, OFC x1, defines the reflection band window in frequency. The periodic reflection bands are determined by the periodic unit cell delay and number of unit cells in the super cell.

Fig. 6 shows a narrower frequency interval of the same response as shown in Fig. 5, demonstrating the null bandwidth variations and the relative change in reflectivity as the super cell length increases. This plot can also be compared to the plot of Fig. 2.

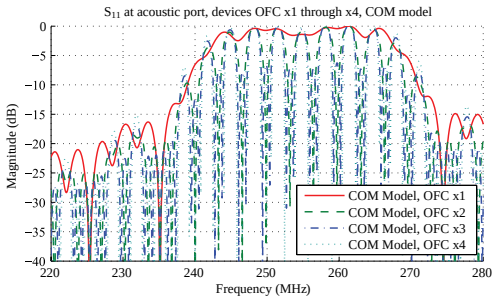

Fig. 5. COM model predicted reflector frequency response of devices OFC x1 through OFC x4 (output is normalized for comparison)

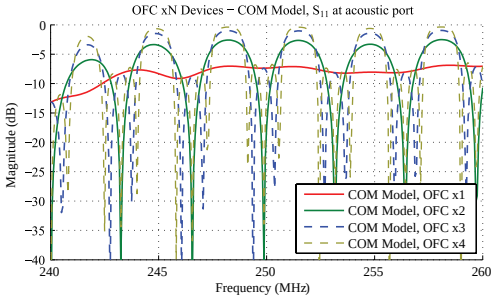

Fig. 6. COM model predicted reflector frequency response of devices OFC x1 through OFC x4 (output is not normalized)

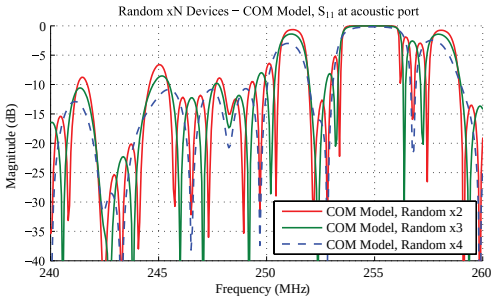

Fig. 7. COM model predicted reflector frequency response of devices RND x1 through RND x4 (output is not normalized), with relative magnitudes

Fig. 7 shows the COM model frequency response for the devices composed of the randomized unit cell. The general positions of peaks and nulls are close to those predicted by the simple model, but the peak around 255MHz is saturated due to the inter- and intra- reflectivity effects, which is not predicted by equation (11). The character of the reflector response is very diversity owing to the uniqueness of the random structure of the unit cell.

V. Measurement and Results

It is not possible to measure acoustic ports of reflector banks (super cells) directly. Data was acquired through a transducer using a network analyzer and then transformed into the time domain using the Fourier transform. The super cell reflection has been gated out in the time domain and transformed back into the frequency domain. The transducer response has been measured separately and compensated for in the response of the super cells. The experimental reflector responses have been compensated, eliminating the transducer response effect, providing the proper reflector magnitude frequency response.

The COM simulation parameters were adjusted slightly to align the frequency nulls (velocity change) and the reflectivity was fixed at the value due to the electrical shorting effect. These model parameters will need further study for these structures, but the transfer function is presently of interest.

Fig. 8 shows the experimental frequency response of OFC x1 through OFC x4 devices. It can be noted that the number of peaks, their relative location, and bandwidths correlate well with theory (Fig. 2) and COM model simulations (Fig. 6).

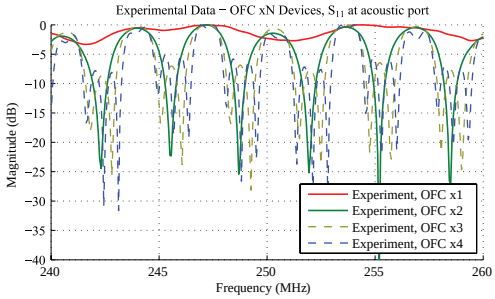

Fig. 8. Experimental reflector frequency response of devices OFC x1 through OFC x4 (output is normalized). This result compares well to the predicted response of Fig. 6.

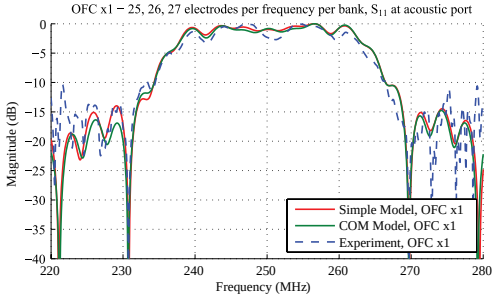

Fig. 9. Predicted reflector frequency response of simple and COM models compared to experimental data for OFC x1 device

Fig. 9 shows the normalized expanded frequency response of device OFC x1, which is a super cell consisting of just one OFC bit. This response represents the unit cell, $H(f)$ in section II. Devices OFC x2, x3, and x4 are expected to generate the desired peaks and nulls within this frequency response window. For this device both models and the data correlate remarkably well.

Fig. 10 shows the frequency response of a super cell consisting of two bits (2-unit cell). At this point both models and experimental data agree with exception at the high frequencies where there appears to be a slight ripple.

Fig. 11 and Fig. 12 show responses of super cells with 3 and 4 bits, respectively. The overall character of the frequency responses is predicted quite well, however, there is a noticeable ripple within the reflection bands. At this point it is not clear

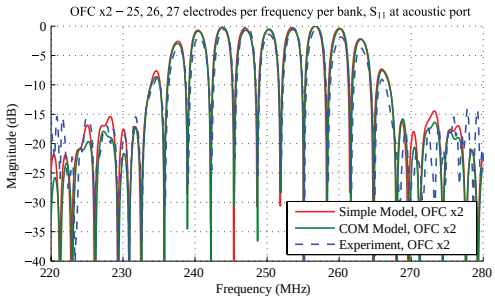

Fig. 10. Predicted reflector frequency response of simple and COM models compared to experimental data for OFC x2 device

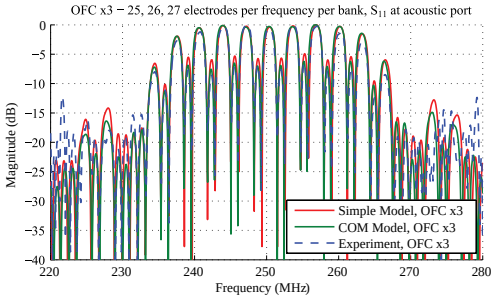

Fig. 11. Predicted reflector frequency response of simple and COM models compared to experimental data for OFC x3 device

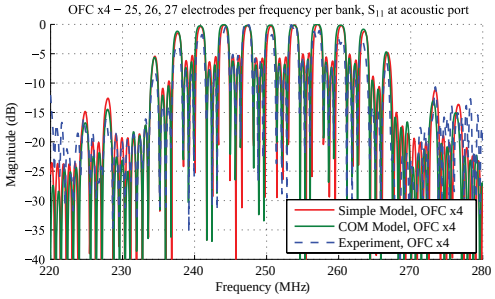

Fig. 12. Predicted reflector frequency response of simple and COM Models compared to experimental data for OFC x4 device

the reason the experimental devices have this ripple. It may be due to the device layout, mode conversion, fabrication, or some other effect. Future research on long super cell structures is required to explain this effect.

Fig. 13 shows the normalized frequency response of device RND x1, which is a unit cell consisting of random, different primitive cells. This corresponds to $H(f)$ in section II. Again, the RND x1 response is expected to act as the frequency window as the super cell increases in length. The comparison of measured and predicted responses is quite good. The response has unique character dependent on the nature of the unit cell, demonstrating the results of the randomized primitive cells.

Fig. 14 shows modeled and measured frequency responses of a super cell consisting of two random unit cells. The nulls and peaks are predicted quite well, but the experimental data

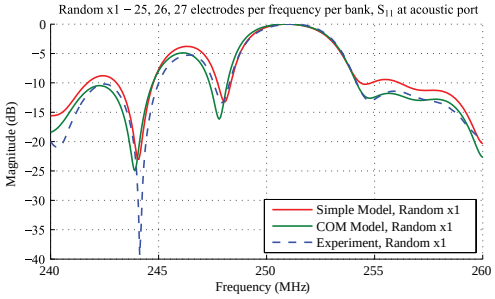

Fig. 13. Predicted reflector frequency response of simple and COM models compared to experimental data for RND x1 device

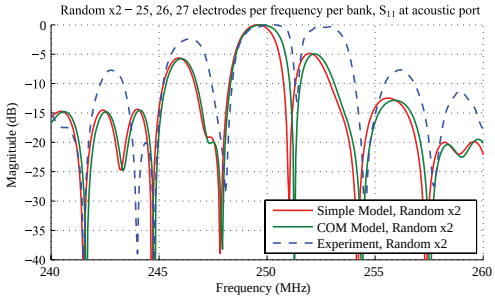

Fig. 14. Predicted reflector frequency response of simple and COM models compared to experimental data for RND x2 device

shows a much stronger reflectivity than predicted, evidenced by the higher side-lobes and broader stop bands.

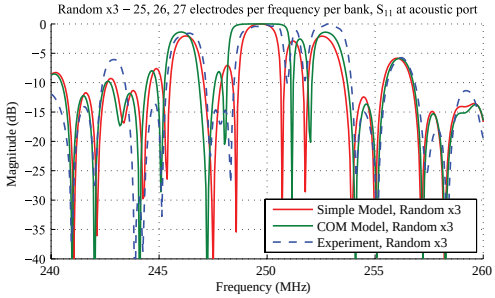

Fig. 15. Predicted reflector frequency response of simple and COM models compared to experimental data for RND x3 device

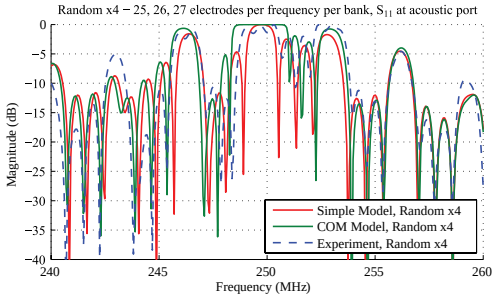

Fig. 16. Predicted reflector frequency response of simple and COM models compared to experimental data for RND x4 device

Fig. 15 and 16 show responses of super cells with 3 and 4 random unit cells, respectively. The general measured frequency response characteristics agree between predictions and measurements is evident; however, there is greater divergence between all the plots. The COM model is much closer to the experimental measurements than the simple model since strong reflectivity can be accounted. It appears that the COM model reflectivity should be decreased which would result in a narrowing of the null spacing and a smoothing of the peak frequency responses but this has not been verified. The 4-cell reflector begins to show ripples, similar to that seen in the OFC 3- and 4-cell structures. At this point it is not clear the reason the experimental devices have this ripple. It may

be due to the device layout, mode conversion, fabrication, or some other effect, again, future research on long super cell structures is required.

VI. Conclusion and Future Work

The purpose of this paper was to present research into new and novel SAW phononic structures. These structures are constructed using well known photolithographic techniques and thin film materials. This paper presents some of the first embodiments we have studied and tries to establish a framework for defining the structures implemented. SAW reflector embodiments were demonstrated that had periodic, pseudo-periodic and random properties in their structural design. Experiments conducted showed that it is possible to design and build structures with multiple stop-bands with near unity reflection. It has also been demonstrated that the preliminary design can be done using a simple model and then fully predicted using the COM model. The simple model can significantly simplify the initial design procedures and provides insight for new direction. The current work examined the structures as reflectors, but similar work needs to be conducted to characterize the transfer function through the grating.

There is still much work to be done on embodiments which would be used for practical applications. Applications for these structures may include device coding, filtering or others. The paper described one dimensional SAW phononic structures, but two and three dimensional structures may offer even greater possibilities, for coding, filtering, waveguiding, etc.

References

[1] C.-S. Kee, J.-E. Kim, H. Y. Park, K. J. Chang, and H. Lim, "Essential role of impedance in the formation of acoustic band gaps," *Journal of Applied Physics*, vol. 87, pp. 1593–1596, Feb. 2000.

[2] S. Yang, J. H. Page, Z. Liu, M. L. Cowan, C. T. Chan, and P. Sheng, "Ultrasound tunneling through 3d phononic crystals," *Physical Review Letters*, vol. 88, no. 10, pp. 104 301–+, Mar. 2002.

[3] V. Laude, M. Wilm, S. Benchabane, and A. Khelif, "Full band gap for surface acoustic waves in a piezoelectric phononic crystal," *pre*, vol. 71, no. 3, pp. 036 607–+, Mar. 2005.

[4] S. Benchabane, A. Khelif, J.-Y. Rauch, L. Robert, and V. Laude, "Evidence for complete surface wave band gap in a piezoelectric phononic crystal," *pre*, vol. 73, no. 6, pp. 065 601–+, Jun. 2006.

[5] A. Khelif, A. Choujaa, S. Benchabane, B. Djafari-Rouhani, and V. Laude, "Guiding and bending of acoustic waves in highly confined phononic crystal waveguides," *Applied Physics Letters*, vol. 84, pp. 4400–+, May 2004.

[6] T.-T. Wu, H.-T. Tang, Y.-Y. Chen, and P.-L. Liu, "Analysis and design of focused interdigital transducers," *Ultrasonics, Ferroelectrics and Frequency Control, IEEE Transactions on*, vol. 52, no. 8, pp. 1384–1392, Aug. 2005.

[7] Y. Nelin, "Apodized phononic crystals," in *Ultrasonics Symposium, 2005 IEEE*, vol. 1, 18-21 Sept. 2005, pp. 62–64.

[8] K.-B. Gu, C.-L. Chang, J.-C. Shieh, and W.-P. Shih, "Design and fabrication of 2d phononic crystals in surface acoustic wave micro devices," in *Micro Electro Mechanical Systems, 2006. MEMS 2006 Istanbul. 19th IEEE International Conference on*, 2006, pp. 686–689.

[9] V. Laude, L. Robert, W. Daniau, A. Khelif, and S. Ballandras, "Surface acoustic wave trapping in a periodic array of mechanical resonators," *Applied Physics Letters*, vol. 89, pp. 3515–+, Aug. 2006.

[10] L. Dhar and J. A. Rogers, "High frequency one-dimensional phononic crystal characterized with a picosecond transient grating photoacoustic technique," *Applied Physics Letters*, vol. 77, pp. 1402–+, Aug. 2000.

[11] D. Malocha, D. Puccio, and D. Gallagher, "Orthogonal frequency coding for SAW device applications," in *Ultrasonics Symposium, 2004 IEEE*, vol. 2, 23-27 Aug. 2004, pp. 1082–1085Vol.2.

[12] B. P. Abbott, "A coupling-of-modes model for SAW transducers with arbitrary reflectivity weighting," Ph.D. dissertation, University of Central Florida, 1989.